Food Chemistry: X 25 (2025) 102207

Contents lists available at ScienceDirect

Food Chemistry: X

journal homepage: www.sciencedirect.com/journal/food-chemistry-x

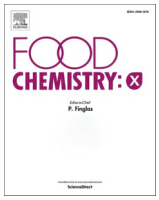

Comparative study of the effects of different lipid oxidation simulation systems on the physicochemical properties of proteins isolated from four cultivated walnut (*Juglans sigillata* Dode) varieties

Wenyun Xiong [a,b,c], Lixin Ding [a,b,c], Wendie Cui [a,b,c], Lei Zhao [d], Shengbao Cai [a,b,c,*]

[a] Faculty of Food Science and Engineering, Kunming University of Science and Technology, Kunming, Yunnan Province 650500, People's Republic of China
[b] Yunnan Engineering Research Center for Fruit & Vegetable Products, Kunming, Yunnan Province 650500, People's Republic of China
[c] Yunnan Key Laboratory of Plateau Food Advanced Manufacturing, Kunming, Yunnan Province 650500, People's Republic of China
[d] Beijing Engineering and Technology Research Center of Food Additives, Beijing Technology and Business University, Beijing 100048, People's Republic of China

ARTICLE INFO

Keywords:
Walnut protein isolation
Proteomics
Oxidation
Interaction
Molecular docking
Molecular dynamics simulations

ABSTRACT

This study aimed to investigate the effects of different lipid oxides on the physicochemical properties of proteins isolated from four walnut cultivars (YBWPI, NQWPI, XXWPI and STWPI). The main proteins in these WPIs are legume B-like and 11S globulin-like, and XXWPI contained the most unique proteins. In three simulation systems, YBWPI showed the greatest changes in carbonyl value, free sulfhydryl value and intrinsic fluorescence intensity. The secondary structure of STWPI changed obviously. NQWPI showed a unique subunit depolymerization, and its solubility and exogenous fluorescence intensity changed significantly, whereas emulsification and particle size of XXWPI changed the most. The 11S globulin-like and cupin type-1 domain-containing protein (A0A833YDI2) have stronger affinities with the key lipid oxides. The radius of gyration and total solvent accessible surface area values of the legumin B-like protein after oxidation reduced obviously. This study may help to better understand the interrelationship between lipid oxides and walnut protein properties.

1. Introduction

Walnuts (*Juglans sigillata* Dode) are known worldwide for their excellent nutritional, health and organoleptic properties, mainly due to their seeds, the walnut kernel. Walnut kernels are rich in fats, ranging from 52 to 70 %, especially unsaturated fatty acids (Martínez et al., 2010; Savage, 2001). In addition, it is also reported that the protein content of defatted walnut flour is over 40 %, and is rich in essential amino acids (Mao & Hua, 2012; Sze-Tao & Sathe, 2000). These components in walnut kernels are not only beneficial to human health, but are also important ingredients in the food industry. However, during food processing and storage, the high content of unsaturated fatty acids in walnut kernels makes them particularly susceptible to the effects of temperature, light and oxygen, which can lead to oxidation reactions such as autoxidation, photo-oxidation, enzymatic oxidation and thermal oxidation. These oxidative processes not only reduce the quality of the oil, but can also affect the properties of the proteins in walnuts. However, proteins from different walnut varieties may have different sensitivities to lipid oxidation products due to differences in their composition and content, which have not been systematically and comparatively studied, and are worthy of further exploration.

There is a growing body of research on how lipid oxidation products affect the physicochemical properties of proteins. Fatty acids, especially unsaturated fatty acids, are susceptible to the formation of lipid hydroperoxides via enzymatic or non-enzymatic pathways, which are highly reactive and can further participate in a variety of secondary reactions to produce a range of degradation chemicals such as aldehydes, ketones, epoxides and polymers (Zhang et al., 2018). These compounds, especially secondary lipid oxidation products, can interact with proteins and lead to protein oxidation, thereby altering their structure and function and affecting the nutritional value and organoleptic quality of foods (Huang, Yan, et al., 2022; Wang et al., 2018). It has been shown that the type and abundance of proteins may be important factors influencing their sensitivity to lipid oxidation

* Corresponding author at: Faculty of Food Science and Engineering, Kunming University of Science and Technology, Kunming, Yunnan Province 650500, People's Republic of China
E-mail address: caikmust2013@kmust.edu.cn (S. Cai).

https://doi.org/10.1016/j.fochx.2025.102207
Received 2 July 2024; Received in revised form 6 January 2025; Accepted 19 January 2025
Available online 22 January 2025

products. For example, previous studies have shown that two indica rice varieties (*Oryza sativa* L.) and two types of kidney beans (*Phaseolus vulgaris* L.) exhibited differential oxidative sensitivity (Bhattacharjee et al., 2023; Rossi et al., 2022). However, there is a paucity of comprehensive research examining the impact of diverse lipid oxidation products on the physicochemical properties of isolated proteins from different cultivated walnut varieties. Moreover, the interactions between major proteins and key lipid oxidation products remain unclear.

Yunnan Province is one of the most significant walnut production regions in China (Zhou et al., 2022). Accordingly, the present study selected four cultivated walnut varieties commonly grown in Yunnan Province for assessment of their protein sensitivity to lipid oxidation products in three different lipid oxidation simulation systems. Additionally, this study employed computer simulation analysis to elucidate the interactions between major proteins and key lipid oxidation products. By conducting a comprehensive comparison of the effects of different lipid oxidation simulation systems on the proteins of various walnut varieties, this study may help to deepen and expand the understanding and knowledge of the relationship between lipid oxidation products and protein properties, especially for walnut proteins. This, in turn, may facilitate the research and development of more effective control strategies to improve the nutritional and functional qualities of walnut protein-related products.

2. Materials and methods

2.1. Materials and reagents

Four cultivated walnut varieties (Yangbi (YB), Niangqing (NQ), Xixiang (XX), and Santai (ST)) were purchased from the local market in Yunnan, China. LA (purity ≥98.0 %), 1-anilino naphthalene-8-sulphonic acid (ANS, purity ≥98.0 %) and LOX (50,000 U/mg) were purchased from Yuanye Biotechnology Co., Ltd. (Shanghai, China). 2,2′-azobis (2-amidopropane) dihydrochloride (AAPH, purity ≥97.0 %) and acrolein (purity ≥98.0 %) were supplied by Aladdin Biochemical Technology Co., Ltd. (Shanghai, China). Guanidine hydrochloride and 2,4-Dinitrophenylhydrazine (DNPH, purity ≥98.0 %) were obtained from Macklin Biochemical Technology Co., Ltd. (Shanghai, China) and Merck Life Sciences (Sigma) (Shanghai, China), respectively. Bradford protein assay kit and 5,5'-Dithiobis (2-nitrobenzoic acid) (DNTB, purity ≥99.0 %) were supplied by Biyuntian Biotechnology Co., Ltd. (Shanghai, China) and Taitan Technology Co., Ltd. (Shanghai, China), repectively. SDS-PAGE (15 %) denaturing acrylamide colored gel rapid preparation kit was obtained from Sangong Bioengineering Co., Ltd. (Shanghai, China), All other chemicals were all of analytical reagent grade.

2.2. Preparation of walnut protein isolate (WPI)

The extraction of WPI from walnut kernels was based on the reported method (Huang et al., 2023) with slight modifications. First, walnut kernels without pellicles were ground and then degreased with petroleum ether (1:20, *w/v*). After filtration, the defatted sample should be volatilized to remove residual petroleum ether. Then, alkaline extraction and acid precipitation were employed to obtain crude WPI. In brief, the defatted walnut powder was mixed with deionized water in a 1:20 ratio (*w/v*), adjusted to pH 11 using 1.0 M NaOH, stirred well for 2 h at room temperature, and then subjected to centrifugation at 10000*g* for 30 min at room temperature to collect the supernatant. Thereafter, the supernatant was adjusted to pH 4.5 using 1.0 M HCl, placed at room temperature for 1 h and then centrifuged at 10000*g* for 30 min to obtain the precipitate. Finally, the precipitate was resuspended in deionized water and adjusted to pH 7.0. The WPI powder was obtained by lyophilization, and stored at −20 °C for further use.

2.3. Identification of the protein composition of four WPIs

For proteomic analysis, 150.0 μg of total protein from each WPI was enzymatically digested at 37 °C for 20 h. The sample was desalted, and the supernatant was used for nanoscale liquid chromatography, followed by detection using the Q-Exactive high-resolution mass spectrometer. Liquid chromatography was performed by using a 0.1 % formic acid aqueous solution (solvent A) and a 0.1 % formic acid/acetonitrile solution (80 % acetonitrile) (solvent B). The chromatographic column used was an Acclaim PepMapTM RSLC (50 μm*150 mm, Thermo Scientific Technology Inc.), equilibrated with 92 % solvent A, and an injection volume of 1.0 μL was used. The elution gradient used was as follows: 0–98 min, 8 %–28 % B; 98–113 min, 28 %–37 % B; 113–117 min, 37 %–100 % B; 117–120 min, 100 % B. After separation by capillary high-performance liquid chromatography, mass spectrometric analysis was performed on a Thermo QE HF mass spectrometer for 120 min in positive ion mode. The mass-to-charge ratios of peptides and peptide fragments were collected, with 20 fragment spectra (MS^2 scans) obtained after each full scan. The scan range was 400–1800, with a first level resolution of 60,000 and a second level resolution of 15,000. The collision energy was set to 28 eV. The mass spectrometry raw files were analyzed using Proteome Discoverer 2.5 software (Thermo Fisher Scientific, Waltham, MA, USA.) for protein identification.

2.4. Preparation of WPI oxidation

The method for simulating the oxidation of proteins in different lipid oxidation simulation systems was based on the method of Zhao et al. (2020) with slight modifications. The hydroperoxides system was as follows: briefly, LA solution (8.09 mM) and LOX solution (3750 U/mL) were added to WPI suspension (50.0 mg/mL, pH 9.0). The reaction was carried out in the dark at 25 °C for 6 h, and then the pH was adjusted to 4.5 followed by centrifugation (10,000 *g*, 10 min). The precipitate was resuspended in deionized water and the pH was adjusted to 7.0. The acrolein oxidation system was carried out according to the methods described by Wang et al. (2018) and Sun et al. (2022). Acrolein (2.0 mM) was mixed with WPI in PBS (pH 7.4), with a protein concentration of 20.0 mg/mL. The acrolein-WPI solution was continuously shaken in a dark environment at 25 °C for 24 h. For the peroxyl radical oxidation system, walnut protein solution was mixed with AAPH at the protein concentration of 20.0 mg/mL and the acrolein concentration of 5.0 mM. The reaction was carried out in the dark at 37 °C for 24 h. After the reaction, each oxidation system was dialyzed by using 7 kDa dialysis bag for 72 h at 4 °C, and then lyophilized for subsequent analysis.

2.5. Analysis of oxidation indicators of WPIs

2.5.1. Carbonyl content

The carbonyl value was determined by the DNPH method described by Huang et al. (2006). The absorbance values of the reaction solution were measured at 370 nm using a SpectraMax M5 microplate reader (Molecular Device, Sunnyvale, CA, USA). The results were then calculated using formula (1), and expressed as the molar amount (nmol) of carbonyl per milligram of soluble protein.

$$\text{Carbonyl con tent (nmol/mg)} = \frac{A_{370} \times 45.45 \times D}{C} \quad (1)$$

where A_{370} is the absorbance at 370 nm, D is the dilution factor, and C is the protein concentration (mg/mL).

2.5.2. Free sulfhydryl group

The content of free sulfhydryl groups was measured by the DTNB method (Ellman method) as described in the previous report (Sun et al., 2022). A SpectraMax M5 microplate reader was employed to record the absorbance value of the reaction solution at 412 nm. The results were

calculated according to formula (2):

$$\text{Free sulfhydryl (nmol/mg)} = \frac{A_{412} \times 73.53 \times D}{C} \quad (2)$$

where A_{412} is the absorbance at 412 nm, C is the protein concentration (mg/mL), and D is the dilution factor.

2.6. Fourier transform infrared (FTIR) spectroscopy

FTIR spectroscopy (Tensor 27, Bruker, Germany) was performed using the KBr tablet method in the wavelength range of 4000–400 cm^{-1}. Data were analyzed using Omnic 8.2 (Thermo Fisher Scientific Inc., Massachusetts, USA) and PeakFit v4.12 (Systat Software Inc., San Jose, California, USA).

2.7. Intrinsic fluorescence spectrum

The intrinsic fluorescence of a WPI solution (0.5 mg/mL) was determined using a SpectraMax M5 microplate reader based on the method of Lei et al. (2021) with slight modifications. Measurement conditions included an excitation wavelength of 283 nm and an emission spectral range of 290–500 nm.

2.8. Exogenous fluorescence spectroscopy

According to the method proposed by Yang et al. (2017), ANS was used as a fluorescent probe to measure the exogenous fluorescence spectrum. WPI was dissolved in PBS (10 mM, pH 8) at a concentration of 0.5 mg/mL, after which a volume of 4.0 mL of the WPI solution was taken and 20.0 μL of 8.0 mM ANS was added. The mixture was then protected from light and stirred for 15 min. Fluorescence intensity was recorded using a SpectraMax M5 microplate reader (excitation wavelength, 365 nm; emission wavelength range, 450–600 nm).

2.9. Sodium dodecyl sulfate–polyacrylamide gel electrophoresis(SDS-PAGE) analysis

The SDS-PAGE gel electrophoresis technique was employed to analyze the samples under reducing conditions. First, the sample solution was mixed with a 5 × reducing protein sample buffer and heated in a water bath at 100 °C for 8 min. The mixture was then immediately transferred to an ice bath and stored at −20 °C for subsequent experiments. Analysis was performed on a Bio-Rad vertical electrophoresis system (Bio-Rad Inc., Hercules, USA) using a 15 % separating gel and a 5 % stacking gel. The stacking gel was first subjected to a voltage of 80 V, which was immediately increased to 120 V upon entry into the separating gel. The gel was stained with the R250 stain for 30 min. Subsequently, the gel was destained and analyzed using a Bio-Rad Gel Imager (Bio-Rad Inc., Hercules, USA). This experiment was repeated three times.

2.10. Particle size measurement

Following the method of Kong et al. (2019), the average particle size and particle size distribution of different samples were determined using a laser particle size analyzer (Malvern Instruments Ltd., Worcestershire, UK). WPI was dissolved in deionized water at a protein concentration of 1.0 mg/mL. All sample measurements were conducted at 25 °C and each result are expressed as the mean and standard deviation (SD) of three replicate experiments.

2.11. Solubility

Following the measurement method of Huang et al. (2022) with slight modifications, proteins were suspended in PBS (10 mM, pH 7.4) at a concentration of 10.0 mg/mL and processed on a shaker at 170 rpm for 2 h at 25 °C, followed by centrifugation at 5000 *g* for 10 min. The protein concentration in the supernatant was determined using the Bradford Protein Assay kit. The data were calculated using formula (3):

$$\text{Solubility} = \frac{\text{Protein concentration in the supernatant (mg/mL)}}{\text{Total protein concentration (10mg/mL)}} \times 100 \quad (3)$$

2.12. Emulsification properties

The determination of the Emulsifying Activity Index (EAI) and the Emulsion Stability Index (ESI) is based on the method of Shi et al. (2023) with slight modifications. Soybean oil and WPI solution (1 % *w/v*) were mixed in a ratio of 1:3 and homogenized at 12000 rpm for 2 min using an IKA T18 homogenizer (IKA Werke GmbH & Co KG, Staufen, Germany). After homogenization and standing for 10 min, 50.0 μL were taken from the bottom and dispersed in 5.0 mL of sodium dodecyl sulphate (SDS, 0.1 % w/v). The absorbance of samples at 0 min (A_0) and 10 min (A_{10}) was measured at 500 nm using a SpectraMax M5 microplate reader, and EAI and ESI were calculated using eqs. (4) and (5), respectively.

$$\text{EAI } (m^2/g) = \frac{2 \times 2.303 \times A_0 \times D}{C \times \Theta \times 10000} \quad (4)$$

$$\text{ESI } (min) = \frac{A_0}{A_0 - A_{10}} \times 10 \quad (5)$$

where D is the dilution factor, C is the WPI concentration (g/mL), Θ is the oil volume fraction, A_0 and A_{10} are the absorbance at 0 min and 10 min, respectively.

2.13. Molecular docking and molecular dynamics (MD) simulation

Based on the proteomics results, five walnut proteins with the highest abundance (about 90 % of the total abundance) were selected for computer simulation with the key lipid oxidation products (13-hydroperoxylinoleic acids (13-HPODEs), acrolein and isobutyl peroxyl radical (iBU) in the three oxidation simulation systems. The protein structures were optimized using GROMACS 19.5 software package, following the download of the 3D structures from AlphaFold (https://alphafold.com/) via the protein Accession number (Fig. S1). Small molecules employed in this study included acrolein (PubChem ID 7847) and 13-HPODEs (PubChem ID 22508268), which were obtained from PubChem (https://pubchem.ncbi.nlm.nih.gov/). IBU are drawn in mol format by MolView (https://molview.org/) and then converted to pdb format using the Open Babel software (open source). The AutoDock 4.2 software (San Diego, CA, USA) was applied to perform blind docking of the optimized structure files with each of the five proteins, and the molecular docking results were analyzed using PyMOL 2.5 (open source, Schrödinger, New York, NY, USA) and the Discovery Studio Visualizer Client (open source, BIOVIA, San Diego, CA, USA). Finally, MD simulations were conducted using the GROMACS 19.5 software package. The detailed procedures are described in a previous report (Zhao et al., 2024). The root mean square deviation (RMSD), radius of gyration (Rg) and total solvent accessible surface area (SASA) were extracted for further analysis.

2.14. Statistical analysis

All experiments were repeated at least three times. Data analysis was conducted using SPSS 26 software (IBM, Chicago, USA). Results are presented as mean ± standard deviation (S.D.) ($n = 3$). In addition, one-way analysis of variance combined with the Tukey test was used to assess significant differences ($p < 0.05$). Figure was performed using Origin 2022 software (OriginLab, Northampton, USA).

3. Results and discussions

3.1. Analysis of protein composition

As a treasure trove of plant proteins, walnuts are rich in protein content and their contribution to human health is self-evident. However, the differences in protein composition among walnut varieties may significantly affect their physicochemical properties, processing and so on, which in turn affect the quality of the final product. Consequently, a comprehensive examination of the protein composition of distinct walnut varieties is of important for investigating the effects of different lipid oxidation simulation systems on their physicochemical properties. In this study, the protein profiles of four walnut varieties, YBWPI, NQWPI, XXWPI and STWPI, were meticulously analyzed by using proteomics methods. As shown in Fig. 1 and Table S1, 384, 483, 423, and 487 types of proteins were identified in the four walnut varieties, respectively. Both shared proteins and unique protein components were identified among the varieties. Specifically, 229 proteins were shared in all four walnut varieties, suggesting a degree of commonality in their protein composition. Among the proteins of these four walnut cultivated varieties, legumin B-like, 11S globulin-like, 11S globulin seed storage protein 2-like, cupin type-1 domain-containing protein, and plant lipid transfer protein were predominant and accounted for about 90 % of the total protein abundance. Meanwhile, the four WPIs also exhibited their unique protein compositions, with two unique proteins in the YBWPI, four unique proteins in the NQWPI and STWPI, and, most notably, 149 unique proteins in the XXWPI, accounting for 35.22 % of their total protein species. In terms of shared protein, the percentage of legumin B-like and 11S globulin-like proteins common to all four walnut varieties exceeded about 50 %, similar to the results of a previous study on other walnut varieties (Zhao et al., 2022). The high percentage of these proteins may not only reflect their structural and functional importance in walnut proteins, but also provides important clues for understanding the common features of walnut proteins. Furthermore, the differences in the types and proportions of other proteins among different species may confer their unique structural and functional properties, particularly in the context of different oxidative conditions (Rossi et al., 2022).

3.2. Oxidation characterization

Based on the proteomics results in the Figure 1and Table S1, it was clearly shown that the protein composition of the WPIs of these four walnut varieties were different. And according to the findings reported earlier (Bhattacharjee et al., 2023; Rossi et al., 2022), the protein differences may lead to their different oxidation behaviors when subjected to lipid oxidation simulation systems. Usually, the oxidative properties of proteins are typically evaluated in terms of carbonyl and free sulfhydryl values (Huang et al., 2006). The carbonyl values are presented in Fig. 2A, which demonstrates that the carbonyl content of all four WPIs was significantly increased at three different oxidation levels in comparison to their respective control ($p < 0.05$). Specifically, in the acrolein-treated group, the carbonyl content of YBWPI, NQWPI, XXWPI and STWPI increased by about 69.93 %, 55.99 %, 42.70 % and 53.96 %, respectively. Similarly, the carbonyl content of YBWPI, NQWPI, XXWPI and STWPI increased by about 82.40 %, 31.08 %, 44.18 % and 40.21 %, respectively, in AAPH-treated group. A similar trend was also observed in the LA + LOX group, where YBWPI, NQWPI and XXWPI exhibited an increase of about 77.16 %, 55.55 % and 26.71 %, respectively, while STWPI showed a significant increase of about 97.20 %. These results highlighted that all four WPIs underwent a significant degree of oxidation after oxidative treatment. However, the extent of oxidative changes varied considerably among the varieties, which may be attributed to their different protein composition (Fig. 1 and Table S1). Previous studies have also demonstrated notable discrepancies in the carbonyl values of proteins isolated from rice and walnut when subjected to the same oxidation simulation system (Li et al., 2020; Sun et al., 2022). These findings are consistent with the those obtained in the current work and serve to further prove that protein compositions may exert a significant influence on their oxidation behaviors. Nevertheless, further investigation may be required to elucidate the relationship between specific protein species and carbonyl value. In addition, the interaction between proteins and free radicals generated by lipid oxidation has the potential to lead to the formation of protein free radicals that are susceptible to attack by molecular oxygen, resulting in the formation of protein peroxides (Zirlin & Karel, 1969). If these peroxides are formed on the α-carbon or other carbons of amino acid residues in proteins, an increase in carbonyl content is an inevitable consequence (Huang et al., 2006). In addition, acrolein readily reacts with nucleophilic groups in proteins, particularly with cysteine, histidine and lysine residues, resulting in structural changes and carbonylation of specific amino acids (Aldini et al., 2011). Conversely, the reaction between peroxide radicals and protein molecules can result in the generation of carbon-centered radicals within the side or main chains of amino acid residues, which may subsequently lead to structural changes and carbonylation (Headlam & Davies, 2004). In the LA + LOX group, the formation of carbonyl groups in WPI may also be due to the transfer of free radicals from oxidized LA to WPI, which can attack the side or backbone of proteins, leading to the degradation of the protein backbone, oxidative

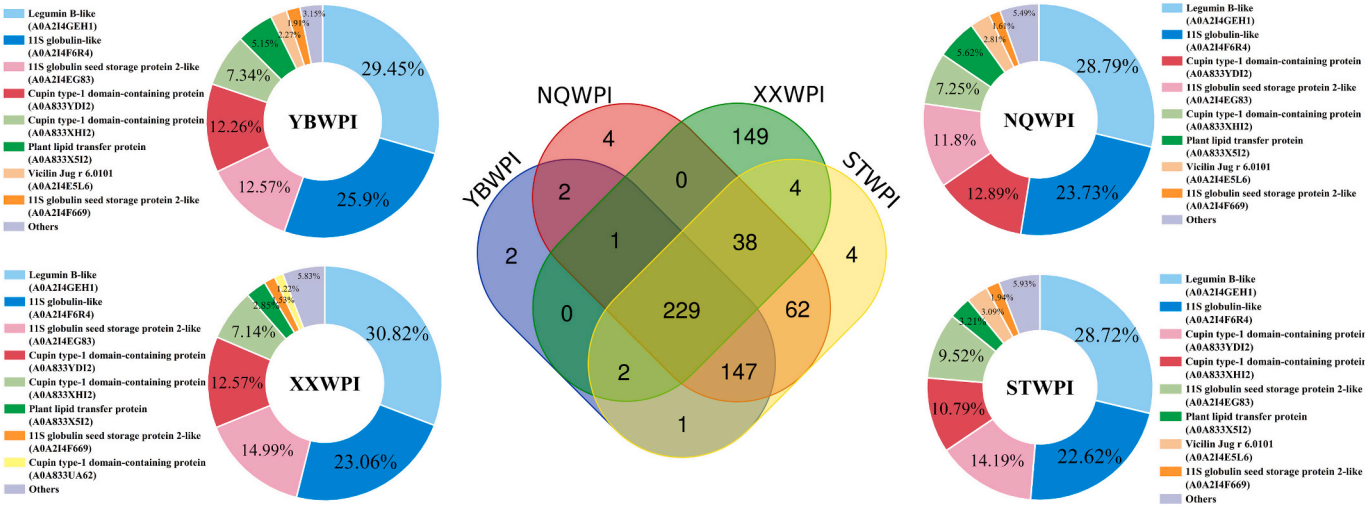

Fig. 1. Identification of the protein composition of YBWPI, NQWPI, XXWPI, and STWPI by proteomics. Yangbi (YB), Niangqing (NQ), Xixiang (XX), and Santai (ST).

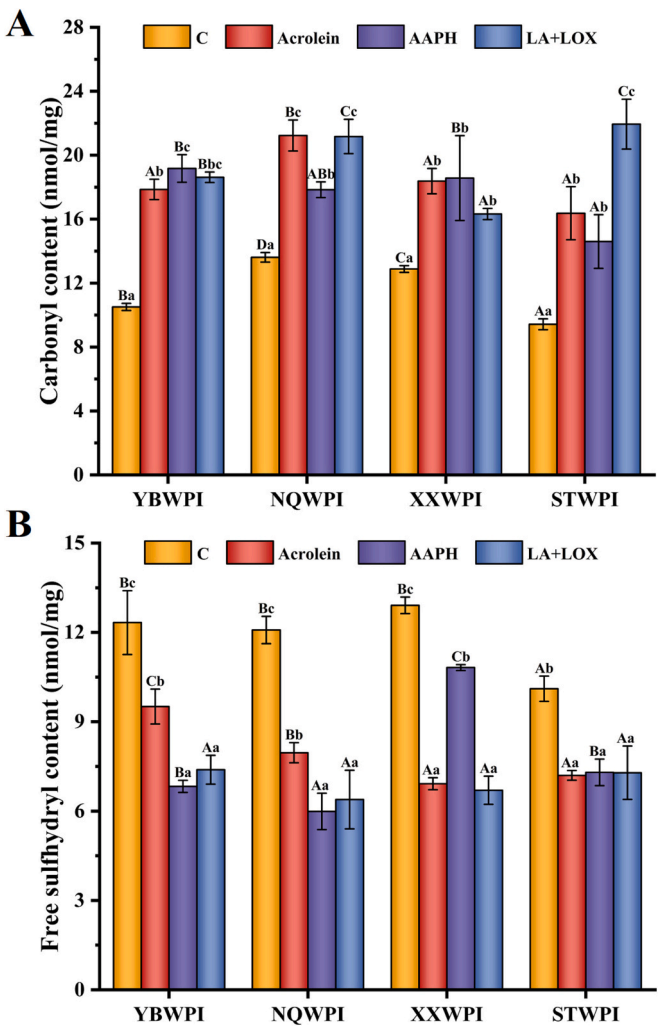

Fig. 2. Carbonyl values (A) and free sulfhydryl values (B) of four WPIs (YBWPI, NQWPI, XXWPI, and STWPI) under three oxidation conditions. All data are expressed as the mean ± SD ($n = 3$). Values with the same letter (a-c) indicate no significant difference in the same protein under different oxidation treatments ($p > 0.05$), or values with the same letters (A, B, C, D) represent no significant difference in different types of WPIs under the same oxidation treatments ($p > 0.05$). Yangbi (YB), Niangqing (NQ), Xixiang (XX), and Santai (ST).

cleavage of the glutamyl side chain, or the reaction with lipid oxidation products, initiating the oxidation process (Zhao et al., 2019).

In numerous instances, cysteine residue is the most sensitive amino acid residue to oxidative conditions in proteins. However, the carbonyl content does not accurately reflect the oxidation status of cysteine residue. Therefore, the free sulfhydryl content was determined using DNTB. Fig. 2B demonstrates the changes of free sulfhydryl values of the four WPIs in the presence of three oxidation systems. The free sulfhydryl values of YBWPI, NQWPI, XXWPI, and STWPI decreased significantly in the presence of the three oxidative systems, with a decrease of about 22.87 %, 34.11 %, 46.40 %, and 28.78 %, respectively, under the acrolein treatment ($p < 0.05$). The values decreased by about 44.61 %, 50.41 %, 16.19 %, and 27.79 % under the AAPH treatment, and by about 40.06 %, 47.10 %, 48.10 %, and 27.89 % under the LA + LOX treatment, respectively. These findings are consistent with those of previous studies in which the free sulfhydryl values of soybean proteins were significantly reduced under similar oxidative conditions (Huang et al., 2006). Additionally, these results indicated that the free sulfhydryl content following oxidation exhibited variability among walnut varieties, potentially attributable to differences in protein composition (Fig. 1 and Table S1). Similarly, previous studies have reported comparable outcomes, whereby the alterations in sulfhydryl values of distinct proteins subjected to an identical oxidation simulation system exhibited a notable discrepancy (Li et al., 2020; Sun et al., 2022). Oxidation may not only alter the redox potential of WPI, but may also affect the equilibrium of the sulfhydryl-disulfide bond exchange reaction, which in turn alters the distribution of free sulfhydryl groups (Huang, Yi, & Fan, 2022). In addition, oxidative modification of neighboring free sulfhydryl groups may lead to the formation of disulfide bonds and other oxidative species, which may trigger protein aggregation and polymerization phenomena (Fu et al., 2019).

The distinct oxidation treatments resulted in a notable increase in the carbonyl content and a reduction in the free sulfhydryl value of all WPIs, which indicates that WPIs were indeed affected by oxidation. In terms of the combined change values of carbonyl and free sulfhydryl, YBWPI exhibited the most pronounced change in the oxidized system, followed by STWPI, NQWPI and XXWPI. These findings indicate that walnut varieties profoundly affect the oxidative properties of their proteins, which may be due to the different composition and proportions of proteins in different walnut varieties.

3.3. Secondary structure analysis by FTIR

Lipid oxidation products affect certain amino acid residues of proteins, which in turn influences the secondary structure of proteins (Aldini et al., 2011). Therefore, FTIR spectroscopy was used to further explore the changes in the secondary structure of proteins in different walnut varieties under different lipid oxidation simulation systems. The alterations in the secondary structure and spatial distribution of proteins under diverse oxidation conditions can be delineated by analyzing the amide I band (1700–1600 cm^{-1}) of the FTIR spectra (Bertram et al., 2006). In contrast, α-helices and β-sheets are regarded as ordered structures within the context of protein secondary structure, whereas random coils and β-turns are considered to be disordered (Zhao et al., 2022). As shown in Fig. 3, acrolein treatment resulted in a reduction in β-turns (by about 9.79 %, 5.57 % and 5.39 %) and an increase in random coils (by about 2.90 %, 2.05 % and 1.48 %) for YBWPI, XXWPI and STWPI, suggesting that the three WPIs exhibited a tendency towards a more compact and ordered protein conformation following acrolein treatment. In the secondary structure of proteins, the amide C═O and N—H groups are typically considered as the main forces to stabilize the α-helical conformation. However, the α-helical decrease of NQWPI and STWPI suggests that acrolein may disrupt the pristine van der Waals interactions between amino acid residues (Wang et al., 2018). AAPH treatment resulted in a consistent trend of decreasing the proportion of α-helices and β-turns while increasing the proportion of β-sheets for the four WPIs, a result similar to previous studies that have demonstrated that peroxyl radicals can disrupt the stabilizing bonds that are essential for maintaining the integrity of the α-helices (Zhao et al., 2022). In the case of the LA + LOX treatment, YBWPI, NQWPI and STWPI showed an increase in β-sheet structure (by about 3.47 %, 4.39 % and 3.33 %), a decrease in β-turn structure (by about 6.32 %, 9.17 % and 14.43 %), while all other structures showed a slight decrease. The XXWPI exhibited a notable degree of variability, with a obvious decrease in β-sheet structure (11.52 %), an increase in random coils (4.14 %), an increase in α-helices (6.98 %) and a decrease in β-turns (3.17 %).

The ratio of α-helices to β-turns of the four WPIs decreased after treatment with different oxidation systems, indicating an increase in the flexibility of the protein and a decrease in the structural regions (Zhao et al., 2022). The structural change exhibited variability across different WPIs, with the most notable variation observed in STWPI, followed by XXWPI, YBWPI, and NQWPI. The most pronounced decrease in β-turn was observed in the AAPH condition for STWPI, while the most pronounced increase in β-turn was observed in the LA + LOX condition for NQWPI. In the LA + LOX conditions, the β-sheet and random coil of XXWPI were increased, whereas the reduction of α-helix of YBWPI was

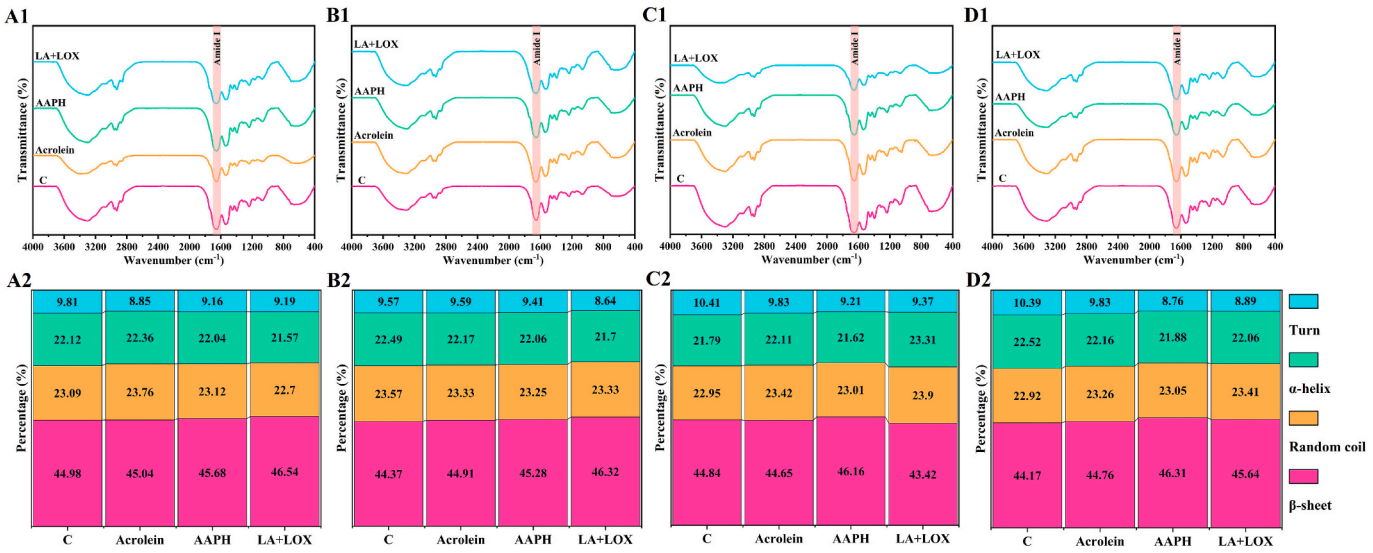

Fig. 3. The FTIR spectra (A1-D1) and secondary structure composition (A2-D2) of different types of WPIs under different oxidation treatments. A-D represent YBWPI, NQWPI, XXWPI, and STWPI. Yangbi (YB), Niangqing (NQ), Xixiang (XX), and Santai (ST).

most significant in all oxidation conditions. The findings indicated that distinct protein types (Fig. 1 and Table S1) may exhibit disparate stability and response characteristics in the context of oxidative stress. Nevertheless, further studies and analysis are required to elucidate which protein contributes the most to the overall change magnitude. Previous studies also exhibited that α-lactalbumin and rice bran proteins had significant differences in the magnitude of secondary structure changes in the same oxidation conditions (Huang, Yi, & Fan, 2022; Zhou et al., 2017).

3.4. *Analysis of intrinsic fluorescence spectrum*

When proteins interact with other molecules, resulting in alterations to their primary and secondary structures, the conformation of the proteins may undergo a change, which can impact the intensity of their intrinsic fluorescence (Jiang et al., 2024). Fig. 4 A1-D1 shows the intrinsic fluorescence spectra. Following the oxidation of acrolein, the fluorescence intensity of YBWPI, XXWPI and STWPI was found to have significantly decreased, by about 21.16 %, 23.45 % and 12.90 %, respectively. In contrast, the fluorescence of NQWPI was increased by about 9.63 %. Following the AAPH treatment, the fluorescence intensity of YBWPI and XXWPI decreased by about 14.22 % and 19.52 %, respectively. In contrast, the fluorescence intensity of NQWPI and STWPI increased by about 28.54 % and 12.96 %, respectively. The maximum endogenous fluorescence intensity of YBWPI (about 31.18 %), NQWPI (about 0.23 %), XXWPI (about 8.04 %), and STWPI (about 8.64 %) was decreased by LA + LOX treatment. In all four WPIs subjected to different oxidative treatments, the observed reduction may be due to protein aggregation, resulting in the burial of exposed tryptophan residues; alternatively, lipid radicals may convert tryptophan to indole, thereby changing the conformation of tryptophan and surrounding aromatic amino acid residues, leading to a decrease in the maximum fluorescence intensity (Wang et al., 2018). However, the maximum intrinsic fluorescence intensity of NQWPI was increased under acrolein

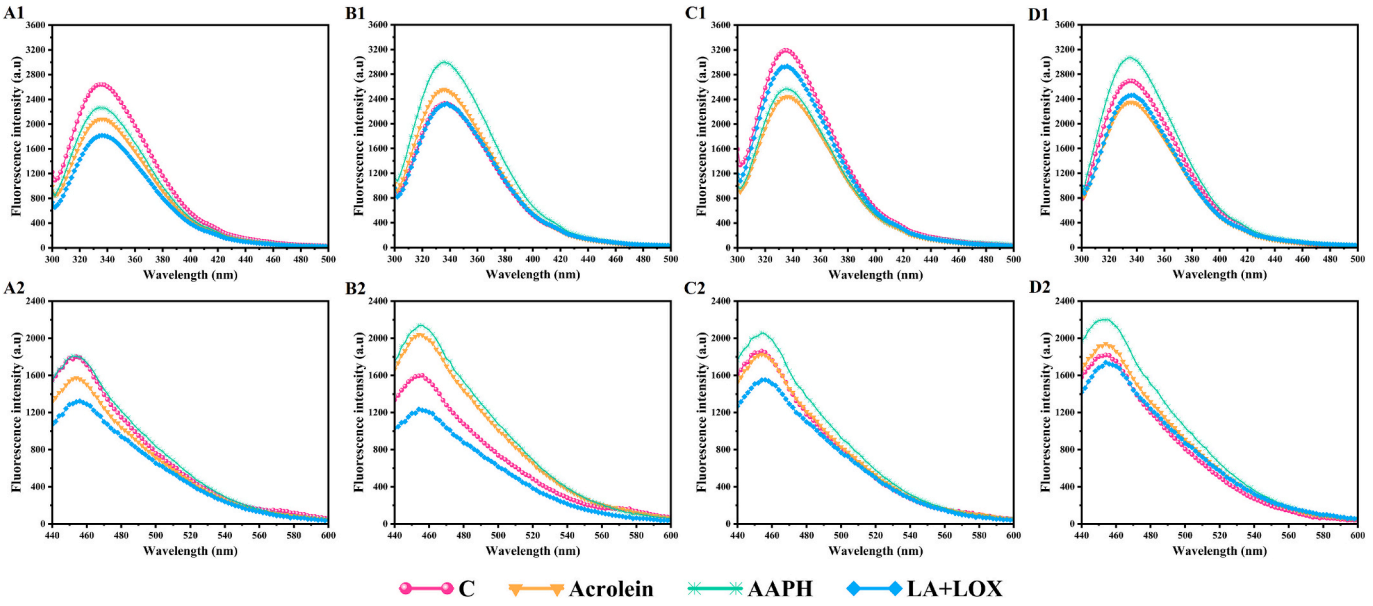

Fig. 4. The intrinsic fluorescence spectra (A1-D1) and exogenous fluorescence spectra (A2-D2) of different types of WPIs under different oxidation treatments. A-D represent YBWPI, NQWPI, XXWPI, and STWPI. Yangbi (YB), Niangqing (NQ), Xixiang (XX), and Santai (ST).

and AAPH treatments, whereas the intrinsic fluorescence intensity of STWPI was also increased under AAPH treatment. This may be due to oxidation-induced depolymerization of the proteins resulting in an increase in the maximum fluorescence intensity, which can be further corroborated by the results of the subsequent SDS-PAGE experiment. The results indicated that the intrinsic fluorescence intensity of different WPIs changed to different degrees after oxidation, which was also potentially attributable to differences in protein composition (Fig. 1 and Table S1). Previous studies also reported that proteins derived from different sources exhibited different changes in their intrinsic fluorescence when subjected to the same oxidation condition (Li et al., 2020; Sun et al., 2022). In addition, among the samples, YBWPI and XXWPI exhibited the greatest variability, with a significant decrease in fluorescence intensity observed under various oxidation conditions; in contrast, NQWPI and STWPI demonstrated unique responses, suggesting the potential involvement of different oxidation mechanisms or intrinsic protective properties, which needs to be investigated in the future.

3.5. Exogenous fluorescence spectrum analysis

In addition to intrinsic fluorescence, the exogenous fluorescence intensity enables the investigation of protein conformational alterations and the evaluation of structural modifications in protein interactions with other molecules. Hydrophobicity is a significant factor in maintaining the tertiary structure of proteins and is essential for protein aggregation and stability (Ma et al., 2022). The light probe ANS has a high affinity for hydrophobic amino acids (in particular, tryptophan) in proteins, and can be used as a fluorescent probe to study the protein conformation, and structural changes (Wang et al., 2008). As shown in Fig. 4 A2-D2, the exogenous fluorescence spectra of the four WPIs showed a maximum intensity at about 454 nm. Following acrolein treatment, the maximum fluorescence intensity of YBWPI and XXWPI decreased by about 12.66 % and 1.02 %, respectively, and an increased by about 27.26 % and 6.40 % for NQWPI and STWPI, respectively. After AAPH treatment, the maximum fluorescence intensity of YBWPI, NQWPI, XXWPI, and STWPI increased by about 0.52 % and 31.14 %, 9.76 % and 20.76 %, respectively. Following co-treatment with LA and LOX, the maximum exogenous fluorescence intensity of the four WPIs, with increases observed in YBWPI (about 26.51 %), NQWPI (about 22.88 %), XXWPI (about 16.06 %), and STWPI (about 4.35 %). The reduction in the maximum exogenous fluorescence intensity following oxidative treatment may be attributed to the hydrophobic amino acids becoming concealed within the protein and the aggregation of the protein structure after oxidation (Li et al., 2023). This finding is consistent with the observed decrease in the endogenous fluorescence intensity. Conversely, the elevation in maximum exogenous fluorescence intensity subsequent to oxidative modification of proteins may be attributed to the exposure of fluorescent groups within the proteins to the aqueous environment, which enhances the probability of fluorescent groups coming into contact with fluorescent probes, thereby resulting in an augmented fluorescence intensity (Ma et al., 2022).

Among these WPIs, the exogenous fluorescence spectra of NQWPI were more easily affected in the three oxidation systems, followed by YBWPI, STWPI and XXWPI. The different changes in exogenous fluorescence spectra of four WPIs may be attributable to the types and content of the proteins they contain (Fig. 1 and Table S1). Previous studies have also reported that the exogenous fluorescence of proteins derived from different sources showed different alternations when subjected to oxidation (Li et al., 2020; Sun et al., 2022). In view of the varying degrees to which exogenous fluorescence is affected in different proteins, future studies could be conducted by purification and separation of these proteins in order to exactly elucidate their specific response mechanisms.

3.6. SDS-PAGE analysis

Cross-linking between protein subunits is a key factor in studying changes in the physicochemical properties of proteins after oxidation. Among many analytical techniques, SDS-PAGE has become an ideal tool to study the oxidative cross-linking of walnut protein subunits due to its significant advantages of fast speed, high resolution, and high sensitivity. As shown in Fig. 5, the molecular weights of the four WPIs were mainly distributed between 15 and 25 kDa, ~35 kDa, and 40–55 kDa

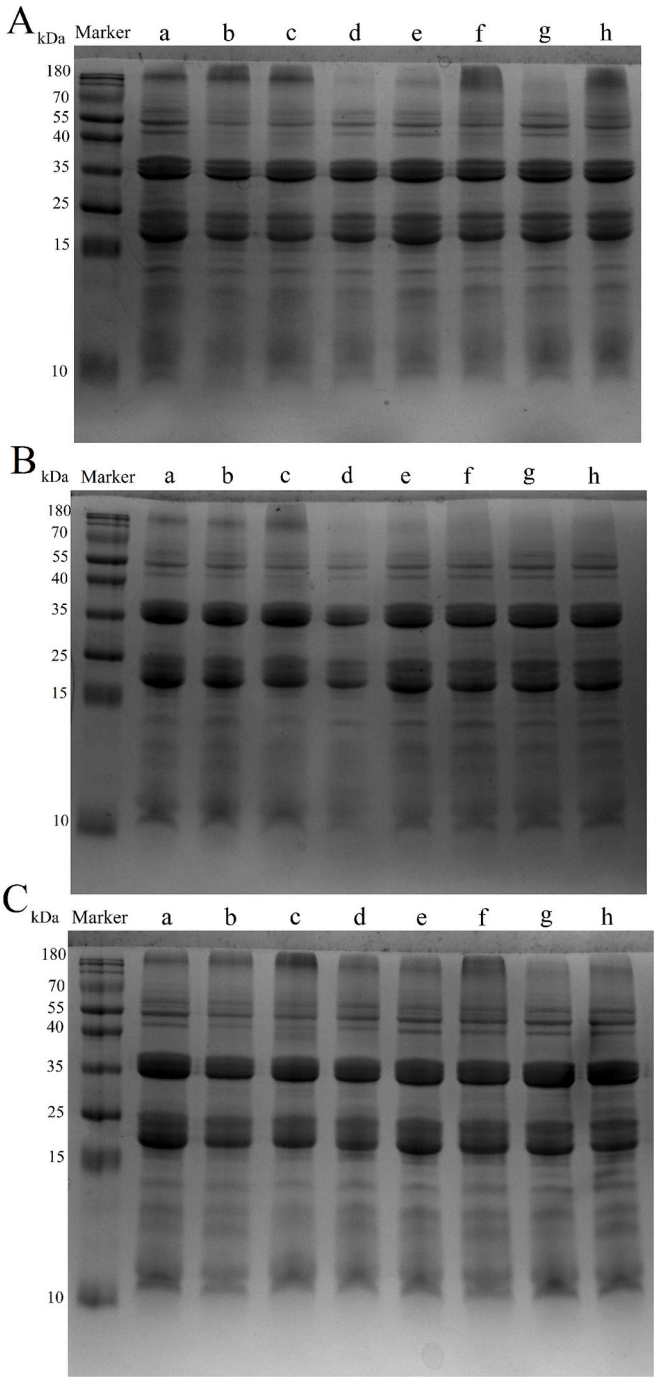

Fig. 5. SDS-PAGE profiles of different types of WPIs under different oxidation treatments. A-C represent the acrolein, AAPH, and LA + LOX groups, respectively. Lanes a-h represent the YBWPI control group, YBWPI treatment group, NQWPI control group, NQWPI treatment group, XXWPI control group, XXWPI treatment group, STWPI control group, and STWPI treatment group. Yangbi (YB), Niangqing (NQ), Xixiang (XX), and Santai (ST).

under reducing conditions. Fig. 5A shows the SDS-PAGE plots of the four WPIs after acrolein treatment, and a new band larger than 180 kDa was observed in YBWPI, XXWPI and STWPI. Since the addition of these proteins to β-mercaptoethanol-containing electrophoresis buffer prior to electrophoresis disrupts the disulfide bonds of WPI, the bands formed are aggregates of non-disulfide bound subunits. Acrolein may be a protein cross-linking agent that promotes protein aggregation. The interaction with proteins is a complex process and involves reactions with several amino acid residues, including lysine, histidine, and cysteine, which form different types of adducts (Wang et al., 2018). These adducts may cause protein interactions that lead to aggregate formation. However, weakening of NQWPI aggregation and deepening of low molecular weight bands were observed after acrolein oxidation, suggesting conformational or structural changes of the protein, which is

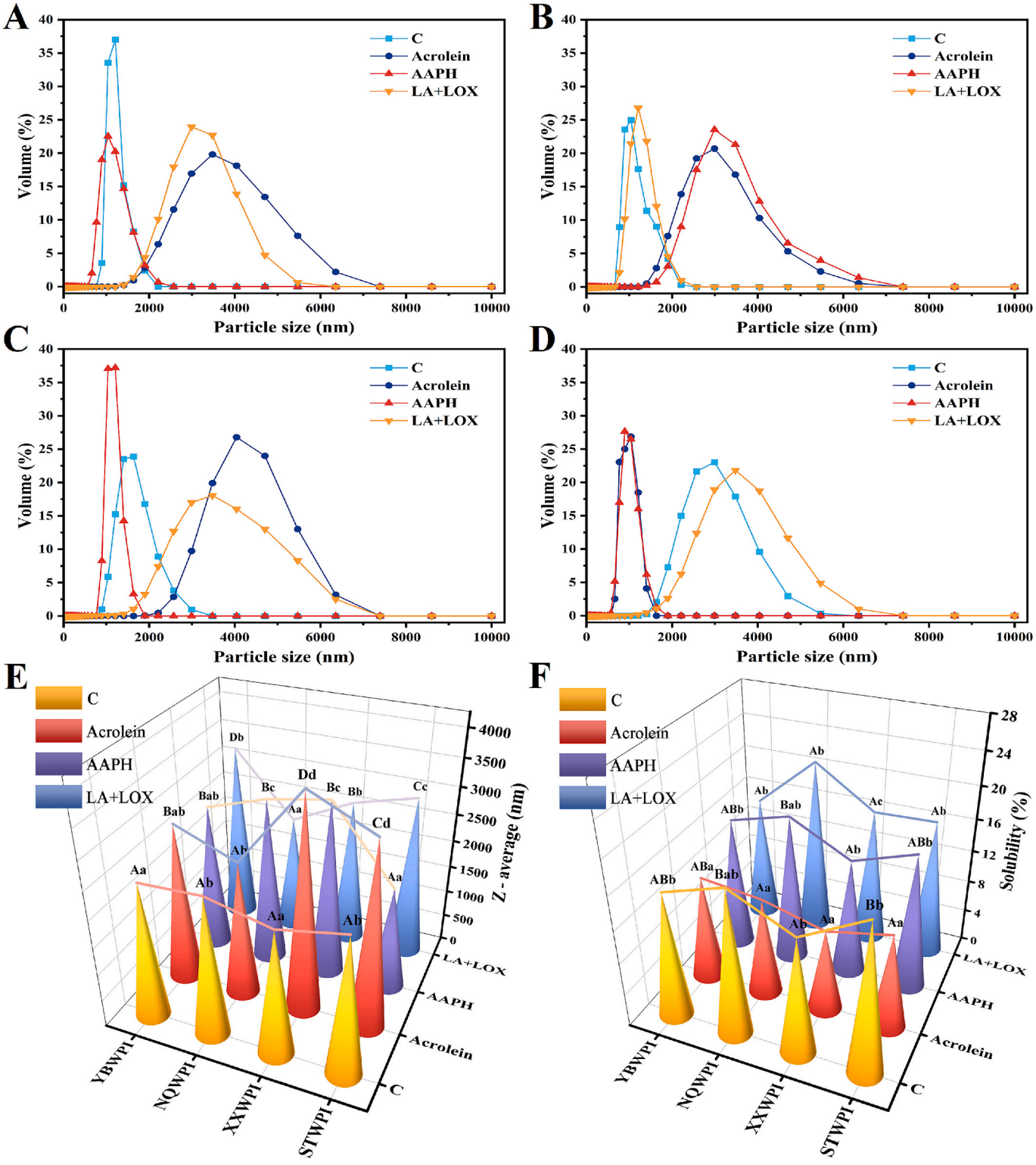

Fig. 6. Particle size distribution (A-D represent YBWPI, NQWPI, XXWPI, and STWPI), average particle size (E), and solubility (F) of four types of WPIs under different oxidation systems. Yangbi (YB), Niangqing (NQ), Xixiang (XX), and Santai (ST).

consistent with the results of enhanced protein depolymerization by endogenous fluorescence intensity of NQWPI after acrolein oxidation.

Fig. 5B shows the SDS-PAGE plot of WPI after oxidation by AAPH. No new bands were observed for YBWPI, XXWPI and STWPI. However, the intensity of the bands for NQWPI and STWPI decreased after oxidation by AAPH, which is consistent with the findings of Dorta et al. regarding peroxyl radical oxidation of myofibrillar proteins (Dorta et al., 2019). The decrease in the intensity of the NQWPI bands was more pronounced after AAPH treatment compared to acrolein treatment. This suggests that 5 mM AAPH treatment leads to a greater degree of depolymerization of WPI compared to 2 mM acrolein, resulting in an increase in endogenous fluorescence intensity.

The SDS-PAGE results of WPIs after co-treatment with LA and LOX are shown in Fig. 5C. The bands of XXWPI and STWPI darkened at >180 kDa, and the darkening of the XXWPI band was more pronounced than that of the STWPI band, whereas the darkening of the YBWPI and NQWPI bands was attenuated. One possible explanation for this aggregation phenomenon is cross-linking between WPI subunits, and another may be the formation of covalent bonds between lipids and proteins, leading to aggregation (Huang et al., 2006). The intensities of the YBWPI and XXWPI bands were significantly reduced at 40–70 kDa, while the intensity of the NQWPI and STWPI bands was slightly increased. Notably, at ~35 kDa, the YBWPI, NQWPI, and XXWPI bands weakened in intensity, while the STWPI bands enhanced in intensity. Results of 15–25 kDa showed a consistent pattern of weakening in all four WPIs. The changes in these bands may reflect the subunit changes of WPI proteins under different treatment conditions, further supporting the mechanism of oxidative and structural changes in WPIs.

3.7. Effect of oxidation on WPI aggregation

3.7.1. Particle size

The particle size and distribution can reveal the state of the protein particles and further understand the effect of oxidation on protein structure and function. The particle size distributions of YBWPI, NQWPI, XXWPI and STWPI are shown in Fig. 6A-D, and the average particle sizes of the four WPIs are shown in Fig. 6E. Analysis of the particle size distributions of the four WPI samples showed that the samples exhibited similar particle size distribution peaks under three different oxidation systems, namely acrolein, AAPH and LA + LOX. Among them, the particle size of YBWPI, NQWPI, XXWPI and STWPI increased by about 16.69 %, 0.59 %, 61.78 % and 35.71 %, respectively, under acrolein treatment; the particle size of YBWPI, NQWPI, XXWPI and STWPI increased by about 6.26 %, 21.72 %, 18.93 % and 18.93 %, respectively, under AAPH treatment. With the LA + LOX combination, the particle sizes of YBWPI, XXWPI and STWPI increased by about 29.71 %, 5.54 % and 24.97 %, respectively, while NQWPI decreased by about 11.91 %. The increase in average protein particle size may be due to protein oxidation, which leads to cross-linking between proteins to form disulfide bonds and protein aggregates (Sante-Lhoutellier et al., 2007). Larger soluble protein aggregates tend to have better stability at the oil/water or air/water interface than smaller protein aggregates (Huang, Yi, & Fan, 2022). And the result of the decrease in particle size is similar to the change in the aggregation of WPI in the SDS-PAGE results. Overall, the change in particle size of XXWPI was most obvious, followed by STWPI, NQWPI, and YBWPI. According to the proteomics results (Fig. 1 and Table S1), XXWPI contained the largest types of unique proteins that may contribute to the different change in protein particle size. This hypothesis requires further investigation to prove.

3.7.2. Solubility

The solubility of proteins depends on their interaction with water, where hydration replaces intramolecular interactions, thereby altering hydrogen bonding and electrostatic forces within the polar regions of proteins (Liu et al., 2019). The impact of oxidized protein aggregates on food quality is an area of great interest in food science. To this end, we investigated the solubility of these oxidized aggregates to assess the effect of protein oxidation on the quality of four WPIs. As shown in Fig. 6F, the protein solubility of four WPIs did not exceed 20 %. Proteomics analysis (see Section 3.1) revealed that the predominant proteins contained in these varieties were legumin B-like (A0A2I4GEH1) and 11S globulin-like (A0A2I4F6R4), which together accounted for approximately 50 % of the total protein content, and both of these proteins belong to the gluten protein family. A previous study have reported that gluten proteins usually have low solubility (Kong et al., 2019), which may explain why the four WPIs had low solubility. Acrolein treatment decreased the solubility of all samples, with STWPI showing the greatest decrease (about 36.17 %), followed by NQWPI (about 32.50 %). With AAPH treatment, while the solubility of STWPI continued to decrease, the other three WPIs showed varying degrees of increase, with NQWPI increasing by about 4.80 %. This indicated that different proteins have different sensitivities to AAPH oxidation. For STWPI, AAPH may lead to structural unfolding and peptide bond breaking, thus reducing solubility; conversely, AAPH may promote the formation of soluble aggregates in other WPIs, thus increasing their solubility. A previous study also reported that AAPH treatment can cause either an increase or a decrease in the solubility of rice bran protein, depending on the degree of oxidation of the proteins (Zhou et al., 2017). This result further supported that the four WPIs had different sensitivities to the AAPH oxidation system, which may be due to differences in their protein composition (Fig. 1 and Table S1). In LA + LOX system, the solubility of NQWPI was significantly increased by about 20.28 % ($p < 0.05$), while YBWPI showed a slight decrease. The changes in solubility and particle size of NQWPI subsequent to oxidation may be attributed to the depolymerization of its proteins following oxidation, which can be proved to some extent by the results of the SDS-PAGE analysis (Fig. 5C).

Based on the above, protein solubility is influenced by the type of oxidation treatment and the intrinsic properties of the protein. NQWPI exhibited the most pronounced solubility changes in response to the different oxidation treatments, thus highlighting its high vulnerability. In contrast, the solubility of STWPI was relatively stable with minimal changes during the different treatments. These findings demonstrate the different responses of WPI to oxidative treatments and provide valuable insights for further studies on the relationship between protein structure and function.

3.8. Emulsification characteristics analysis

Emulsification properties can be used as an important indicator to differentiate the quality characteristics of proteins from different walnut varieties, where EAI reflects the ability of proteins to form emulsions and ESI describes the ability of proteins to maintain the stability of emulsions. By oxidizing the WPI of different walnut varieties and comparing the changes in EAI and ESI, differences in the emulsification properties of WPIs from different varieties subjected to oxidation can be identified.

As shown in Fig. 7, the emulsification properties of all four WPIs decreased under the treatment of three oxidation systems (acrolein, AAPH, LA + LOX). Among them, the EAI of YBWPI, NQWPI, XXWPI and STWPI decreased by about 6.92 %, 24.52 %, 14.32 % and 25.83 %, respectively, after acrolein treatment; by about 17.11 %, 3.82 %, 28.37 % and 26.01 %, respectively, after AAPH treatment; and by about 20.53 %, 3.42 %, 43.55 % and 37.32 %, respectively, by LA + LOX co-treatment. These data suggest that changes in protein solubility and structure, among others, that occur after oxidative treatment have a significant negative impact on the emulsifying capacity of WPI. Previous studies have shown that oxidation induced by peroxyl radicals also leads to a decrease in the emulsification capacity of α-whey proteins, and that moderate oxidation may help to unfold the protein structure, exposing more hydrophobic amino acid residues, facilitating the formation of soluble aggregates, and decreasing the ability of the protein to absorb fat, ultimately leading to a decrease in EAI (Huang, Yi, & Fan, 2022).

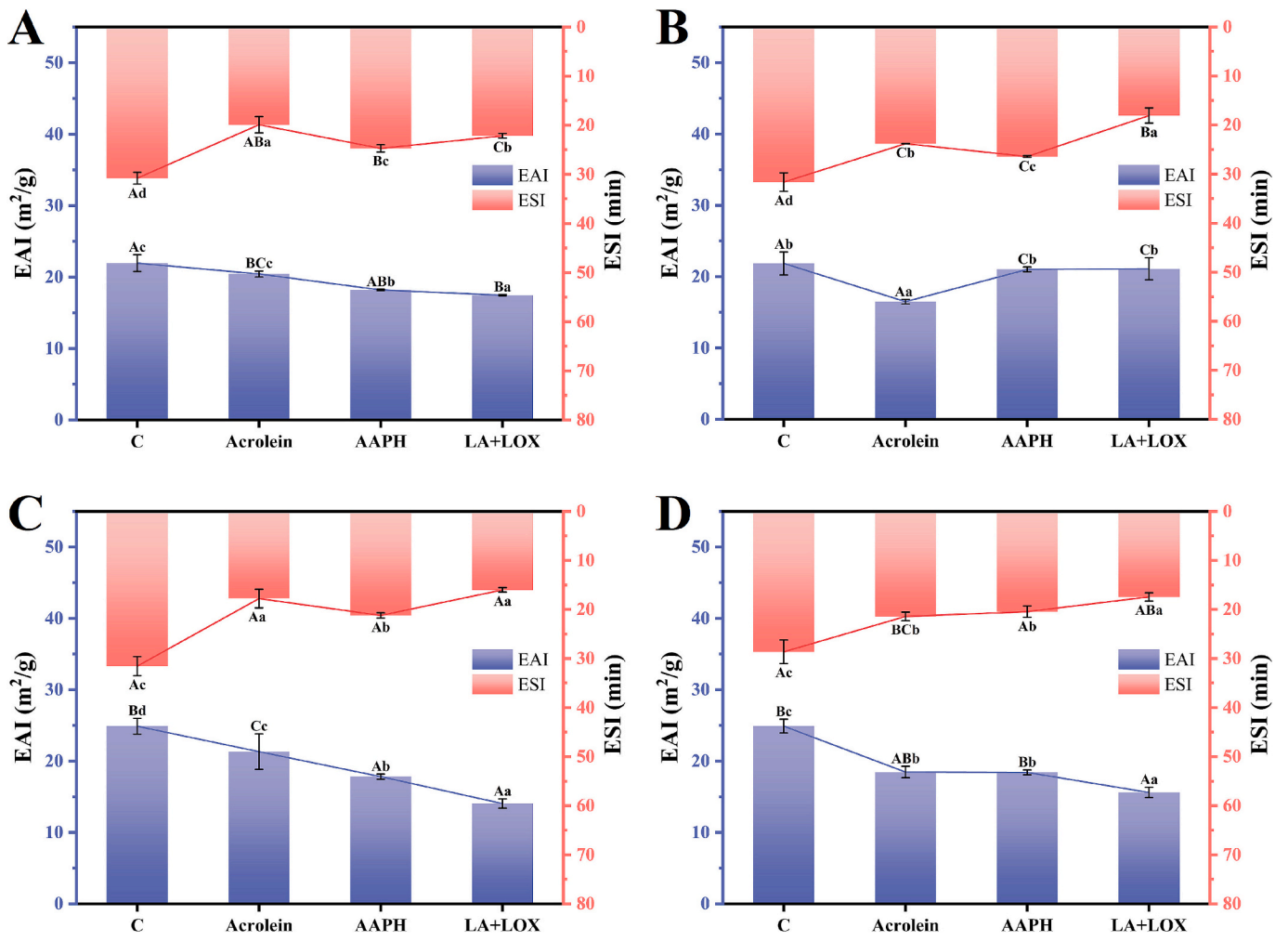

Fig. 7. Emulsifying activity index (EAI) and emulsion stability index (ESI) of four WPIs (A-D represent YBWPI, NQWPI, XXWPI, and STWPI), Different letters (a, b, c) indicating the same type of WPI under different oxidation treatments or different letters (A, B, C) indicating the different types of WPIs under the same oxidation treatment were statistically significant ($p < 0.05$). Yangbi (YB), Niangqing (NQ), Xixiang (XX), and Santai (ST).

Similarly, ESI was also affected by oxidative treatments, YBWPI, NQWPI, XXWPI, and STWPI decreased by about 35.35 %, 24.75 %, 43.64 %, and 25.20 %, respectively, after acrolein treatment; by about 19.72 %, 16.49 %, 32.76 %, and 28.59 %, respectively, after AAPH treatment; and by about 28.01 %, 42.89 %, 49.21 %, and 39.04 %, respectively, after LA + LOX treatment, similar to the previous results of protein ESI decrease after oxidation (Sun et al., 2022). The combined decrease in EAI and ESI suggests that protein oxidation not only impairs the initial EAI, but also affects the ESI formed by WPI.

According to the above results, XXWPI had the most significant decrease in emulsification properties under all oxidative treatments, whereas NQWPI was less affected by oxidative conditions. These results suggested that the emulsification characteristics of WPIs from different walnut cultivars under oxidizing conditions varied considerably, which may be related to their unique protein composition (Fig. 1 and Table S1) or/and their different sensitivities to oxidation.

3.9. Interaction of lipid products with major proteins by computer simulation

In order to gain a deeper insight into the interactions between the major walnut proteins and the key lipid oxidation products, molecular docking and MD simulation were conducted. Fig. 8, panels A1-A5, illustrate the 3D binding site maps of three small molecules (13-HPODEs, acrolein, and iBU) in relation to the proteins legumin B-like (A0A2I4GEH1), 11S globulin-like (A0A2I4F6R4). The 11S globulin seed storage protein 2-like (A0A2I4EG83), cupin type-1 domain-containing protein (A0A833YDI2) and cupin type-1 domain-containing protein (A0A833XHI2), respectively, demonstrated that the binding sites were distinct. The interaction between 13-HPODEs (A6–10), acrolein (A11–15) and iBU (A16–20) with amino acid residues of five major proteins was predominantly facilitated by van der Waals bonds, hydrogen bonds and hydrophobic interactions. These interaction patterns were analogous to those previously observed between the lipid oxidation product *trans*, *trans*-2,4-decadienal (2,4-DEC) and myoglobin (Mb) (Qi et al., 2024). The results of the affinity score analysis (Table S2) showed that 11S globulin-like and cupin type-1 domain-containing protein (A0A833YDI2) exhibited a markedly stronger interaction with the three key lipid oxidation products in comparison to the other three proteins. This indicated that the functional groups of these two proteins may be particularly susceptible to attack by lipid oxidation products. A previous study has found that lipid oxidation products can easily react with nucleophilic groups of proteins (Aldini et al., 2011). Molecular docking results showed that three key lipid oxidation products can interact with a range of amino acids in proteins, including lysine, arginine, aspartic acid, and phenylalanine. It may therefore be hypothesized that key lipid oxidation products may attack these amino acids and alter their structures, thereby leading to changes in the secondary structure of proteins.

In order to gain a deeper understanding of the dynamic changes in

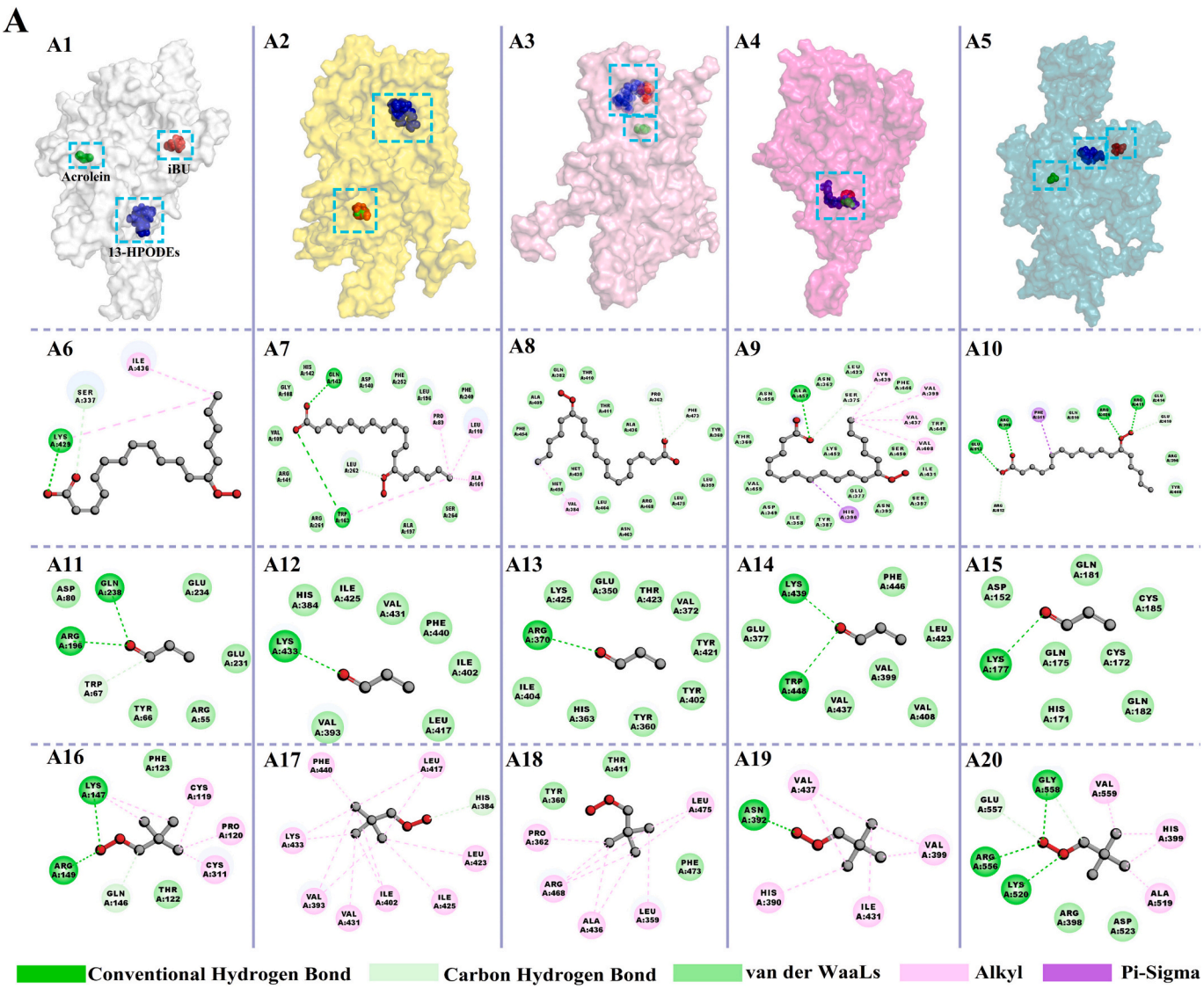

Fig. 8. Results of molecular docking (A) and molecular dynamics (MD) (B) simulations of five major walnut proteins with three key lipid oxidation products. A1–5 represent the 3D binding site maps of three small molecules (13-HPODEs, acrolein, and iBU) with the proteins legumin B-like, 11S globulin-like), 11S globulin seed storage protein 2-like, cupin type-1 domain-containing protein (A0A833YDI2) and cupin type-1 domain-containing protein. A6–10, A11–15, and A16–20 depict the 2D interaction maps of these five proteins with 13-HPODEs, acrolein, and iBU, respectively. B1–5, B6–10, and B11–15 show the root mean square deviation (RMSD), radius of gyrations (Rg), and total solvent accessible surface area (SASA) of the proteins after interacting with the key lipid oxidation products.

protein structural properties induced by lipid oxidation products, MD simulation was employed. The effects of three lipid oxidation products on the RMSD (Fig. 8 B1–5), Rg (Fig. 8 B6–10) and total SASA (Fig. 8 B11–15) of proteins during the interaction process are shown in Fig. 8B and Table S3. The RMSD is often used to evaluate whether a complex system has reached a stable state (Qi et al., 2024). The legumin B-like, 11S globulin seed storage protein 2-like and cupin type-1 domain-containing protein (A0A833YDI2) were able to reach equilibrium relatively quickly upon binding of the three key lipid oxidation products, whereas 11S globulin-like and cupin type-1 domain-containing protein (A0A833XHI2) took relatively longer time to reach equilibrium upon interaction with 13-HPODEs. However, all systems reached a relatively stable state during 100 ns of MD simulation. Rg is employed to describe the distribution of individual atoms of a molecule with respect to the centre of mass of the molecule. It can be used to characterize the compactness of a protein's conformation (Rout et al., 2021). The Rg values of legumin B-like upon binding to acrolein or iBU decreased, suggesting the possibility of aggregation. Similarly, the cupin type-1 domain-containing protein (A0A833YDI2) exhibited comparable alteration in its Rg following its interaction with acrolein. In contrast, the Rg values in the remaining simulation systems were observed to increase, indicating a unfolding process of proteins. The Rg values suggested that the three key lipid oxidation products exert disparate influences on the tertiary structure of the major walnut proteins, which may be a contributory factor to the observed different changes in fluorescence intensities of the various WPIs (Fig. 4). The total SASA of proteins is a key indicator for describing the degree of contact between protein and solvent, and is essential for understanding its physicochemical and functional properties, especially solubility (Qi et al., 2024). Among those five major walnut proteins, the total SASA of legumin B-like underwent a obvious decrease after binding to three key major lipid oxidation products, indicating its solubility may decrease, which is consistent to some extent with the results of the decrease in the solubility of some WPIs after oxidation. The current study provided some insight into how the three key lipid oxidation products interacted with the five major walnut proteins under a relative a simple circumstance. However,

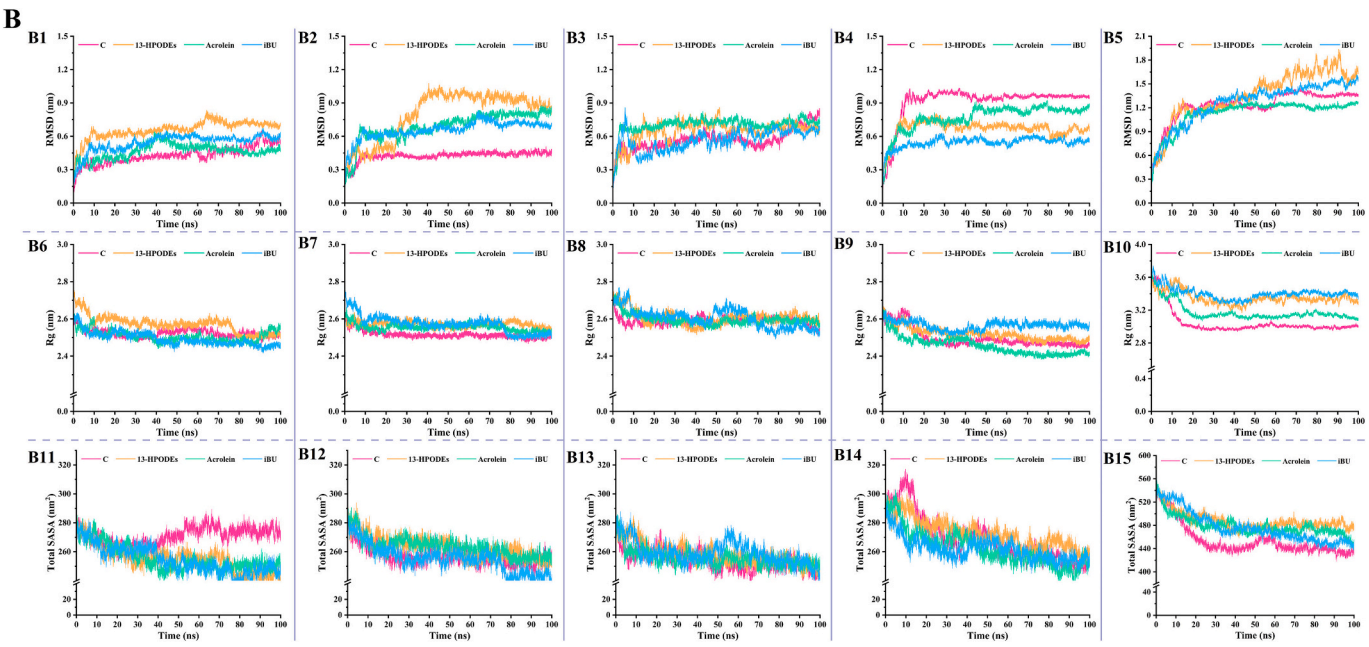

Fig. 8. (*continued*).

during the actual process of lipid oxidation, many complex peroxyl radicals and other secondary oxidation products are produced and formed a very complex oxidation system, which may interact with proteins in a more complex manner (Gou et al., 2024). Some more studies are needed to reveal the interactions between proteins and lipid oxidation products under a complex system in the future.

4. Conclusions

YBWPI, NQWPI, XXWPI and STWPI contained 384, 483, 423 and 487 proteins, respectively, of which XXWPI had the 149 specific proteins. The main proteins in these four WPIs were legumin B-like and 11S globulin-like. After treatment with the three lipid oxidation simulation systems, the carbonyl group values of the four WPIs were increased and the sulfhydryl group values were decreased, and the changes of YBWPI were the greatest. The change in intrinsic fluorescence intensity of YBWPI was also the largest. The secondary structures of the STWPI changed more obviously. Among the four WPIs, the changes in solubility and exogenous fluorescence intensity of NQWPI were the largest, and SDS-PAGE analysis showed that it showed a unique depolymerization of subunits after oxidation, whereas the other three WPIs tended to form aggregates. Particle size analysis showed that XXWPI had the greatest change after oxidation, and its emulsification characteristics were also greatly altered. Molecular docking revealed that, among the five major proteins, 11S globulin-like and cupin type-1 domain-containing protein (A0A833YDI2) have stronger affinities with the key lipid oxidation products. MD results showed that the Rg and SASA values of legumin B-like protein after oxidation reduced obviously, which might be one of the reasons for the decreased solubility of some WPIs subjected to oxidation. Results obtained in the current work may help to deepen the understanding and knowledge of the interaction relationship between lipid oxidation products and walnut proteins, which may facilitate the research and development of more effective control strategies to improve the nutritional and functional qualities of walnut protein-related products. However, the current work was performed under the simulation systems with a relatively simple circumstance, and changes of different walnut protein-related products in real-world situations need to be comprehensively investigated in the future.

CRediT authorship contribution statement

Wenyun Xiong: Writing – original draft, Methodology, Investigation, Formal analysis, Data curation. **Lixin Ding:** Software, Methodology. **Wendie Cui:** Methodology. **Lei Zhao:** Validation, Methodology. **Shengbao Cai:** Writing – review & editing, Validation, Supervision, Conceptualization.

Declaration of competing interest

The authors declare that they have no known competing financial interests or personal relationships that could have appeared to influence the work reported in this paper.

Acknowledgments

This work was financially supported by Major Science and Technology Projects in Yunnan Province (Grant nos.202202AE090007 and 202202AG050009).

Appendix A. Supplementary data

Supplementary data to this article can be found online at https://doi.org/10.1016/j.fochx.2025.102207.

Data availability

Data will be made available on request.

References

Aldini, G., Orioli, M., & Carini, M. (2011). Protein modification by acrolein: Relevance to pathological conditions and inhibition by aldehyde sequestering agents. *Molecular Nutrition & Food Research, 55*(9), 1301–1319. https://doi.org/10.1002/mnfr.201100182

Bertram, H. C., Kohler, A., Böcker, U., Ofstad, R., & Andersen, H. J. (2006). Heat-induced changes in myofibrillar protein structures and myowater of two pork qualities. A combined FT-IR spectroscopy and low-field NMR relaxometry study. *Journal of Agricultural and Food Chemistry, 54*(5), 1740–1746. https://doi.org/10.1021/jf0514726

Bhattacharjee, S., Chakrabarty, A., Kora, D., & Roy, U. K. (2023). Hydrogen peroxide induced antioxidant-coupled redox regulation of germination in rice: Redox

metabolic, transcriptomic and proteomic evidences. *Journal of Plant Growth Regulation, 42*(2), 1084–1106. https://doi.org/10.1007/s00344-022-10615-3
Dorta, E., Ávila, F., Fuentes-Lemus, E., Fuentealba, D., & López-Alarcón, C. (2019). Oxidation of myofibrillar proteins induced by peroxyl radicals: Role of oxidizable amino acids. *Food Research International, 126*, Article 108580. https://doi.org/10.1016/j.foodres.2019.108580
Fu, Q., Liu, R., Wang, H., Hua, C., Song, S., Zhou, G., & Zhang, W. (2019). Effects of oxidation in vitro on structures and functions of myofibrillar protein from beef muscles. *Journal of Agricultural and Food Chemistry, 67*(20), 5866–5873. https://doi.org/10.1021/acs.jafc.9b01239
Gou, F., Gao, S., & Li, B. (2024). Lipid-induced oxidative modifications decrease the bioactivities of collagen hydrolysates from fish skin: The underlying mechanism based on the proteomic strategy. *Foods, 13*(4), 583. https://doi.org/10.3390/foods13040583
Headlam, H. A., & Davies, M. J. (2004). Markers of protein oxidation: Different oxidants give rise to variable yields of bound and released carbonyl products. *Free Radical Biology and Medicine, 36*(9), 1175–1184. https://doi.org/10.1016/j.freeradbiomed.2004.02.017
Huang, H., Yi, J., & Fan, Y. (2022). Influence of peroxyl radical-induced oxidation on structural characteristics, emulsifying, and foaming properties of α-lactalbumin. *LWT- Food Science and Technology, 163*, Article 113590. https://doi.org/10.1016/j.lwt.2022.113590
Huang, X., Yan, C., Lin, M., He, C., Xu, Y., Huang, Y., & Zhou, Z. (2022). The effects of conjugation of walnut protein isolate with polyphenols on protein solubility, antioxidant activity, and emulsifying properties. *Food Research International, 161*, Article 111910. https://doi.org/10.1016/j.foodres.2022.111910
Huang, X., Yan, C., Xu, Y., Ling, M., He, C., & Zhou, Z. (2023). High internal phase emulsions stabilized by alkaline-extracted walnut protein isolates and their application in food 3D printing. *Food Research International, 169*, Article 112858. https://doi.org/10.1016/j.foodres.2023.112858
Huang, Y., Hua, Y., & Qiu, A. (2006). Soybean protein aggregation induced by lipoxygenase catalyzed linoleic acid oxidation. *Food Research International, 39*(2), 240–249. https://doi.org/10.1016/j.foodres.2005.07.012
Jiang, M., Chen, P., Wang, X., Zhu, W., & Wu, J. (2024). Effect of ultrasonic vacuum drying on the structural characteristics of whole-egg protein powder. *LWT- Food Science and Technology, 191*, Article 115490. https://doi.org/10.1016/j.lwt.2023.115490
Kong, X., Zhang, L., Lu, X., Zhang, C., Hua, Y., & Chen, Y. (2019). Effect of high-speed shearing treatment on dehulled walnut proteins. *LWT- Food Science and Technology, 116*, Article 108500. https://doi.org/10.1016/j.lwt.2019.108500
Lei, Y., Gao, S., Xiang, X., Li, X., Yu, X., & Li, S. (2021). Physicochemical, structural and adhesion properties of walnut protein isolate-xanthan gum composite adhesives using walnut protein modified by ethanol. *International Journal of Biological Macromolecules, 192*, 644–653. https://doi.org/10.1016/j.ijbiomac.2021.10.022
Li, B.-B., Cao, Z.-Y., Zhang, W., Wei, S., Lv, Y.-Y., & Hu, Y.-S. (2023). Protein oxidation-induced changes in the aggregation behavior and structure of gluten. *LWT- Food Science and Technology, 184*, Article 115062. https://doi.org/10.1016/j.lwt.2023.115062
Li, F., Wu, X., & Wu, W. (2020). Effects of malondialdehyde-induced protein oxidation on the structural characteristics of rice protein. *International Journal of Food Science & Technology, 55*(2), 760–768. https://doi.org/10.1111/ijfs.14379
Liu, J., Li, P., Jiang, Z., Yang, R., & Zhang, W. (2019). Characterisation of peanut protein concentrates from industrial aqueous extraction processing prepared by spray and freeze drying methods. *International Journal of Food Science & Technology, 54*(5), 1597–1608. https://doi.org/10.1111/ijfs.14028
Ma, Z., Chi, Y., Zhang, H., Chi, Y., & Ma, Y. (2022). Inhibiting effect of dry heat on the heat-induced aggregation of egg white protein. *Food Chemistry, 387*, Article 132850. https://doi.org/10.1016/j.foodchem.2022.132850
Mao, X., & Hua, Y. (2012). Composition, structure and functional properties of protein concentrates and isolates produced from walnut (*Juglans regia* L.). *International Journal of Molecular Sciences, 13*(2), 1561–1581. https://doi.org/10.3390/ijms13021561
Martínez, M. L., Labuckas, D. O., Lamarque, A. L., & Maestri, D. M. (2010). Walnut (*Juglans regia* L.): Genetic resources, chemistry, by-products. *Journal of the Science of Food and Agriculture, 90*(12), 1959–1967. https://doi.org/10.1002/jsfa.4059
Qi, J., Yang, X., Cui, Y., Zhang, Y., Luo, X., Mao, Y., Xu, B., Zhu, L., & Liang, R. (2024). Multispectral and molecular dynamics study on the impact of trans, trans-2,4-decadienal and 4-hydroxy-2-nonenal on myoglobin redox stability. *Food Chemistry, 433*, Article 137366. https://doi.org/10.1016/j.foodchem.2023.137366
Rossi, G. B., Seraglio, S. K. T., Honaiser, T. C., Toaldo, I. M., Costa, A. C. D. O., Faria, J. C., & Arisi, A. C. M. (2022). Protein profile and antioxidant capacity of processed seeds from two common bean (*Phaseolus vulgaris* L.) cultivars. *International Journal of Food Science & Technology, 57*(7), 3934–3943. https://doi.org/10.1111/ijfs.15537
Rout, J., Swain, B. C., Subadini, S., Mishra, P. P., Sahoo, H., & Tripathy, U. (2021). Conformational dynamics of myoglobin in the presence of vitamin B12: A spectroscopic and in silico investigation. *International Journal of Biological Macromolecules, 192*, 564–573. https://doi.org/10.1016/j.ijbiomac.2021.10.030
Sante-Lhoutellier, V., Aubry, L., & Gatellier, P. (2007). Effect of oxidation on in vitro digestibility of skeletal muscle myofibrillar proteins. *Journal of Agricultural and Food Chemistry, 55*(13), 5343–5348. https://doi.org/10.1021/jf070252k
Savage, G. P. (2001). Chemical composition of walnuts (*Juglans regia* L.) grown in New Zealand. *Plant Foods for Human Nutrition, 56*(1), 75–82. https://doi.org/10.1023/A:1008175606698
Shi, L. S., Yang, X. Y., Gong, T., Hu, C. Y., Shen, Y. H., & Meng, Y. H. (2023). Ultrasonic treatment improves physical and oxidative stabilities of walnut protein isolate-based emulsion by changing protein structure. *LWT- Food Science and Technology, 173*, Article 114269. https://doi.org/10.1016/j.lwt.2022.114269
Sun, L., Wu, Q., & Mao, X. (2022). Effects of oxidation modification by malondialdehyde on the structure and functional properties of walnut protein. *Foods, 11*(16), 2432. https://doi.org/10.3390/foods11162432
Sze-Tao, K. W. C., & Sathe, S. K. (2000). Walnuts (*Juglans regia* L): Proximate composition, protein solubility, protein amino acid composition and protein in vitro digestibility. *Journal of the Science of Food and Agriculture, 80*(9), 1393–1401. https://doi.org/10.1002/1097-0010(200007)80:9<1393: AID-JSFA653>3.0.CO;2-F
Wang, X.-S., Tang, C.-H., Li, B.-S., Yang, X.-Q., Li, L., & Ma, C.-Y. (2008). Effects of high-pressure treatment on some physicochemical and functional properties of soy protein isolates. *Food Hydrocolloids, 22*(4), 560–567. https://doi.org/10.1016/j.foodhyd.2007.01.027
Wang, Z., He, Z., Gan, X., & Li, H. (2018). The effects of lipid oxidation product acrolein on the structure and gel properties of rabbit meat myofibrillar proteins. *Food Biophysics, 13*(4), 374–386. https://doi.org/10.1007/s11483-018-9543-6
Yang, X., Li, Y., Li, S., Oladejo, A. O., Ruan, S., Wang, Y., … Ma, H. (2017). Effects of ultrasound pretreatment with different frequencies and working modes on the enzymolysis and the structure characterization of rice protein. *Ultrasonics Sonochemistry, 38*, 19–28. https://doi.org/10.1016/j.ultsonch.2017.02.026
Zhang, Q., Wan, C., Wang, C., Chen, H., Liu, Y., Li, S., Lin, D., Wu, D., & Qin, W. (2018). Evaluation of the non-aldehyde volatile compounds formed during deep-fat frying process. *Food Chemistry, 243*, 151–161. https://doi.org/10.1016/j.foodchem.2017.09.121
Zhao, J., Han, M., Wu, Q., Mao, X., Zhang, J., & Lu, Z. (2022). Effect of oxidative modification by peroxyl radical on the characterization and identification of oxidative aggregates and in vitro digestion products of walnut (*Juglans regia* L.) protein isolates. *Foods, 11*(24), 4104. https://doi.org/10.3390/foods11244104
Zhao, J., Su, G., Zhao, M., & Sun, W. (2019). Physicochemical changes and in vitro gastric digestion of modified soybean protein induced by lipoxygenase catalyzed linoleic acid oxidation. *Journal of Agricultural and Food Chemistry, 67*(50), 13978–13985. https://doi.org/10.1021/acs.jafc.9b05843
Zhao, J., Wu, J., Chen, Y., Zhao, M., & Sun, W. (2020). Gel properties of soy protein isolate modified by lipoxygenase-catalyzed linoleic acid oxidation and their influence on pepsin diffusion and in vitro gastric digestion. *Journal of Agricultural and Food Chemistry, 68*(20), 5691–5698. https://doi.org/10.1021/acs.jafc.0c00808
Zhao, S., Cai, S., Ding, L., Yi, J., Zhou, L., Liu, Z., & Chu, C. (2024). Exploring the blood glucose-lowering potential of the umami peptides LADW and EEAEGT derived from tuna skeletal myosin: Perspectives from α-glucosidase inhibition and starch interaction. *Foods, 13*(2), 294. https://doi.org/10.3390/foods13020294
Zhou, L., Zhang, Y., Zhao, C., Lin, H., Wang, Z., & Wu, F. (2017). Structural and functional properties of rice bran protein oxidized by peroxyl radicals. *International Journal of Food Properties*, 1–12. https://doi.org/10.1080/10942912.2017.1352596
Zhou, X., Peng, X., Pei, H., Chen, Y., Meng, H., Yuan, J., Xing, H., & Wu, Y. (2022). An overview of walnuts application as a plant-based. *Frontiers in Endocrinology, 13*. https://doi.org/10.3389/fendo.2022.1083707
Zirlin, A., & Karel, M. (1969). Oxidation effects in a freeze-dried gelatin-methyl linoleate system. *Journal of Food Science, 34*(2), 160–165. https://doi.org/10.1111/j.1365-2621.1969.tb00910.x